



**HAL**  
open science

# Carbonate-containing apatite (CAP) synthesis under moderate conditions starting from calcium carbonate and orthophosphoric acid

Doan Pham Minh, Ngoc Dung Tran, Ange Nzihou, Patrick Sharrock

► **To cite this version:**

Doan Pham Minh, Ngoc Dung Tran, Ange Nzihou, Patrick Sharrock. Carbonate-containing apatite (CAP) synthesis under moderate conditions starting from calcium carbonate and orthophosphoric acid. *Materials Science and Engineering: C*, 2013, 33 (5), p. 2971-2980. 10.1016/j.msec.2013.03.023 . hal-01632392

**HAL Id: hal-01632392**

**<https://hal.science/hal-01632392v1>**

Submitted on 20 Oct 2018

**HAL** is a multi-disciplinary open access archive for the deposit and dissemination of scientific research documents, whether they are published or not. The documents may come from teaching and research institutions in France or abroad, or from public or private research centers.

L'archive ouverte pluridisciplinaire **HAL**, est destinée au dépôt et à la diffusion de documents scientifiques de niveau recherche, publiés ou non, émanant des établissements d'enseignement et de recherche français ou étrangers, des laboratoires publics ou privés.

# Carbonate-containing apatite (CAP) synthesis under moderate conditions starting from calcium carbonate and orthophosphoric acid

Doan Pham Minh <sup>a,\*</sup>, Ngoc Dung Tran <sup>a</sup>, Ange Nzihou <sup>a</sup>, Patrick Sharrock <sup>b</sup>

<sup>a</sup> Université de Toulouse, Mines Albi, CNRS, Centre RAPSODEE, Campus Jarlard, F-81013 Albi cedex 09, France

<sup>b</sup> Université de Toulouse, SIMAD, IUT Paul Sabatier, Avenue Georges Pompidou, 81104 Castres, France

## A B S T R A C T

The synthesis of carbonate-containing apatite (CAP) from calcium carbonate and orthophosphoric acid under moderate conditions was investigated. In all cases, complete precipitation of orthophosphate species was observed. The reaction temperature influenced strongly the decomposition of calcium carbonate and therefore the composition of formed products. The reaction temperature of 80 °C was found to be effective for the complete decomposition of calcium carbonate particles after 48 h of reaction. Infra-red spectroscopy (IR), nuclear magnetic resonance (NMR), thermogravimetry/mass spectroscopy (TG-MS) coupling, and X-ray diffraction (XRD) characterizations allowed the identification of the composition of formed products. By increasing the reaction temperature from 20 °C to 80 °C, the content of A-type CAP increased and that of B-type CAP decreased, according to the favorable effect of temperature on the formation of A-type CAP. The total amount of carbonate content incorporated in CAP's structure, which was determined by TG-MS analysis, increased with the reaction temperature and reached up to 4.1% at 80 °C. At this temperature, the solid product was mainly composed of apatitic components and showed the typical flat-needle-like structure of CAP particles obtained in hydrothermal conditions. These results show an interesting one-step synthesis of CAP from calcium carbonate and orthophosphoric acid as low cost but high purity starting materials.

### Keywords:

Apatite

One-step synthesis

Calcium carbonate

Orthophosphoric acid

## 1. Introduction

The principal mineral composition of bones and teeth consists of apatite-based compounds, and among them calcium hydroxyapatite (Ca-HA,  $\text{Ca}_{10}(\text{PO}_4)_6(\text{OH})_2$ ) is considered as the main component. In addition, bones and teeth also contain substituted apatites with the presence of other elements including  $\text{Na}^+$ ,  $\text{Mg}^{2+}$ ,  $\text{Cl}^-$ ,  $\text{F}^-$  and  $\text{CO}_3^{2-}$  [1]. Calcium carbonate-containing apatite (CAP) is considered as the major impurity, which is formed by the replacement of  $\text{PO}_4^{3-}$  and/or  $\text{OH}^-$  groups in Ca-HA's structure by  $\text{CO}_3^{2-}$  groups [2,3]. Ca-HA has been considered as a prominent biomaterials for bone and dental tissue reconstitution for its excellent bioactivity with hard tissues, but recently, substituted Ca-HA such as CAP has been found to be more effective with a shorter post-operative rehabilitation program [4–6]. Thus, CAP base materials attract much attention and the awareness of the contribution of CAP to bone and dental enamel health is increasing [7].

Much work has been devoted to the preparation of CAP, which generally consists of the precipitation of orthophosphate anions by calcium cations in aqueous solution in the presence of  $\text{CO}_3^{2-}$  anions [8–10], or the heating of a calcium phosphate at high temperature under a flux of  $\text{CO}_2$  [11,12]. By solution reactions, a mixture of water soluble salts is usually used to enhance the insertion of  $\text{CO}_3^{2-}$  anions in the apatitic

structure. This leads to supplementary washing steps for the elimination of counter ions in order to purify final solid products. Washing steps may be arduous when nano-particles of calcium phosphates are formed, accompanied by the formation of waste by-products containing all counter ions. The heating route relates to a multi-step synthesis in rigorous conditions of temperature and pressure. By this way, a mixture of calcium phosphate (for example, tricalcium phosphate ( $\text{Ca}_3(\text{PO}_4)_2$ ), or calcium pyrophosphate ( $\text{Ca}_2\text{P}_2\text{O}_7$ )), lime (CaO) and/or calcium carbonate ( $\text{CaCO}_3$ ) is heated under  $\text{CO}_2$  atmosphere [12–14].

The present study reports a simple one-step synthesis of CAP from calcium carbonate and orthophosphoric acid under moderate conditions of temperature and pressure. Calcium carbonate was chosen as the source of both calcium cations and carbonate anions, and orthophosphoric acid was chosen as the most effective orthophosphate for the dissolution of calcium carbonate powder particles. Their wide availability and low cost also constitute advantages for an eventual industrialization of the synthesis process.

## 2. Materials and methods

Calcite powder ( $\text{CaCO}_3$ , 98%) with particles of volume-mean diameter of 23.3  $\mu\text{m}$  from Fisher Scientific and orthophosphoric acid ( $\text{H}_3\text{PO}_4$ , 85 wt.% in water) from Merck were used as received, without further modification. The synthesis was carried out in a 250 mL stainless steel reactor (Top Industrial). The reactor was equipped with an

\* Corresponding author. Tel.: +33 563493258; fax: +33 563493043.

E-mail address: doan.phamminh@mines-albi.fr (D. Pham Minh).

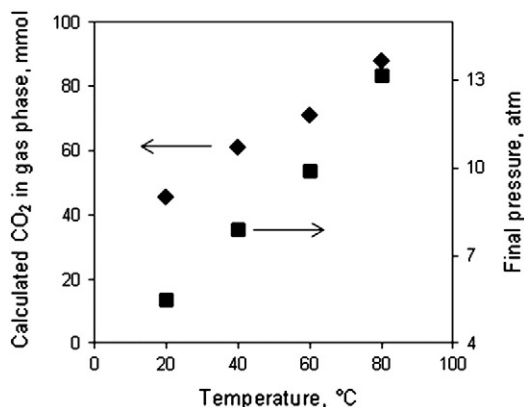


Fig. 1. Quantity of the carbon dioxide at the end of the reaction estimated from gas phase using the ideal gas law and final pressure as a function of the reaction temperature.

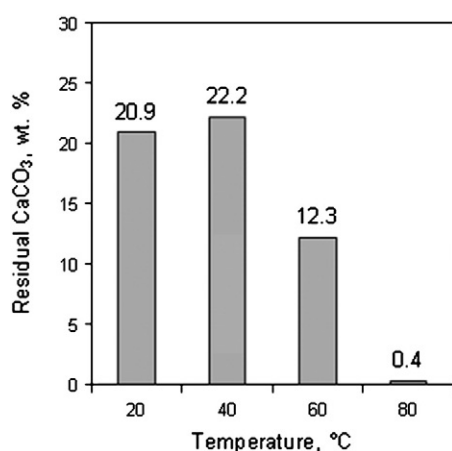


Fig. 2. Content of residual calcium carbonate in the solid products after 48 h of reaction.

electrical heating jacket and a magnetic stirrer. For each reaction, 10 g of  $\text{CaCO}_3$  and 45 mL of water were fed into the reactor. After closing, 6.9 g of  $\text{H}_3\text{PO}_4$  was quickly injected into the reactor by an injection valve and the reaction started by adjustment of the stirring rate at 800 rpm. During the reaction, the reactor was thermostated at the selected temperatures in the range of 20–80 °C for 48 h. After reaction, solid phase was separated from liquid phase by filtration using 0.45  $\mu\text{m}$  filter paper. Then the solid products were dried at 50 °C for 48 h before further characterizations.

Different analysis and characterization techniques were used for studying both solid and liquid phases. Elemental analysis was carried out using inductively coupled plasma atomic emission spectroscopy (ICP-AES) with a HORIBA Jobin Yvon Ultima 2 apparatus. X-ray diffraction (XRD) of the solids was performed using a Philips PANalytical X'pert Pro MPD diffractometer with a  $\text{Cu K}\alpha$  (1.543 Å) radiation source. Thermogravimetry (TG) was performed in a TA Instruments SDTQ600 analyzer with a heating rate of 5 °C  $\text{min}^{-1}$  under air flux (100 mL  $\text{min}^{-1}$ ). Exhaust gases from the TG analyzer outlet were analyzed by a Pfeiffer Vacuum OmniStar GSD 320 mass spectrometer which acquires mass spectra from 0 to 200 amu (atomic mass unit). Diffuse reflection infrared Fourier transform (DRIFT) spectra were recorded on a Shimadzu FTIR 8400S spectrometer on ground solid powders.  $^{31}\text{P}$  and  $^1\text{H}$  NMR spectra were registered on a Bruker Avance 400, operating at 10 kHz for both  $^{31}\text{P}$  and  $^1\text{H}$  NMR at room temperature (21 °C). The adsorption–desorption isotherm was determined with a MICROMETRICS ASAP 2010 using nitrogen as gas adsorbate with the data collection from relative pressure ( $P/P^0$ ) of 0.03 to 0.99. True density of the solid powders was measured by helium pycnometry using an Accupyc 1330 (Micromeritics). Scanning electron microscopy (SEM) was measured on a Philips XL30 ESEM apparatus (FEI Company). Particle size distribution was measured by laser scattering in a Mastersizer 2000 (Malvern Instruments Ltd., Malvern, UK) in the range from 0.020 to 2000  $\mu\text{m}$ .

CAP obtained at 80 °C with the highest calcium carbonate decomposition was formed into cylindrical disks using a hydraulic press, with no additives. The disks were immersed in simulated body fluid (Tris-SBF-27 mM) made according to the method of Jalota et al.

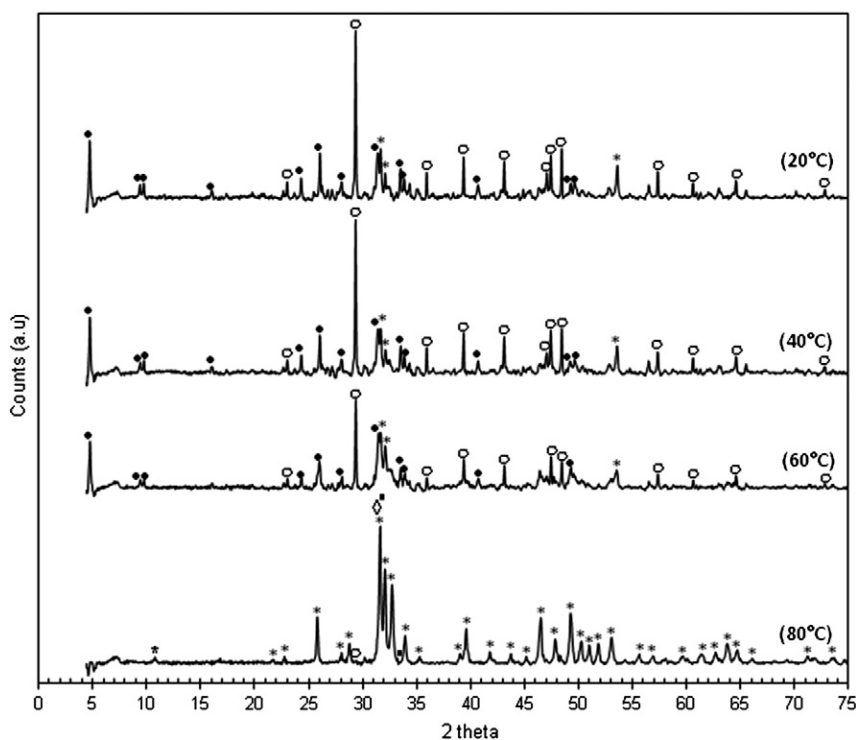


Fig. 3. XRD patterns of the solid products; (\*) OCP (JCPDS standard no. 00-026-1056); (\*) Ca-HA (JCPDS standard no. 01-072-1243); (\*) B-type CAP (JCPDS standard no. 00-004-0697); (◊) A-type CAP (JCPDS standard no. 00-035-0180); and (○) calcite (JCPDS standard no. 00-047-1743).

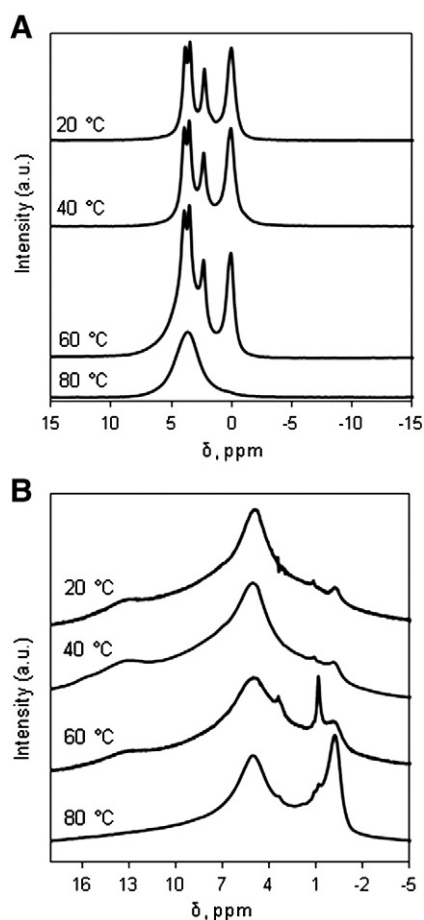


Fig. 4.  $^{31}\text{P}$  NMR (A) and  $^1\text{H}$  NMR (B) spectra of the dried solid products.

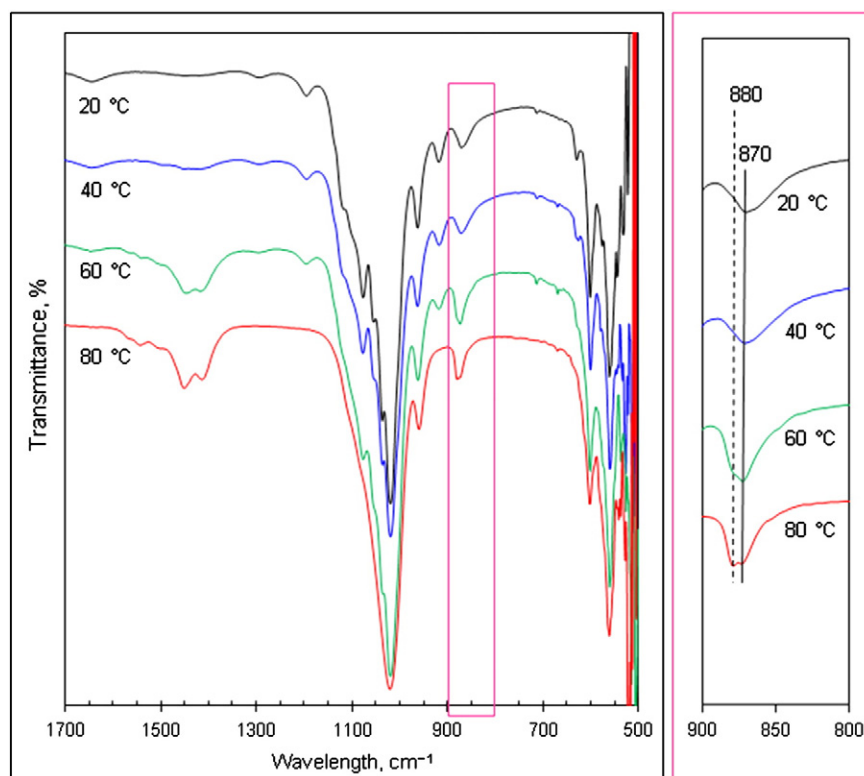


Fig. 5. IR spectra of the solid products; dotted tick: peak position of C–O stretching of A-type CAPs ( $880\text{ cm}^{-1}$ ); and continuous tick: peak position of C–O stretching of B-type CAPs ( $870\text{ cm}^{-1}$ ).

[15]. Following seven days of incubation at  $37\text{ }^\circ\text{C}$ , the samples were rinsed with distilled water, dried at  $37\text{ }^\circ\text{C}$  and observed with SEM analysis technique in order to examine the growth of new calcium phosphate on the surface of CAP disks.

### 3. Results and discussion

#### 3.1. Orthophosphate precipitation and calcium carbonate dissolution

When  $\text{H}_3\text{PO}_4$  was injected into the suspension of  $\text{CaCO}_3$ , the reaction started immediately as observed by the evolution of the pressure in the batch reactor. In all cases, the pressure quickly increased for the first 10 min. Then it slowly increased and stabilized up to the end of the reaction. In the temperature range investigated, the partial pressure of water vapor was close to the atmospheric pressure (approximately 1 bar) so the increase of the pressure could be attributed to the formation of the carbonic gas as shown in Eq. (1).



Carbon dioxide from Eq. (1) could be in gas phase or dissolved in liquid phase. The quantity of carbon dioxide in gas phase could be estimated using the ideal gas law and taking into account the volume of the reactor occupied by the solid and liquid phases and the partial pressure of water vapor at the corresponding temperature (Fig. 1).

Both final pressure and quantity of carbon dioxide in gas phase linearly increased with the reaction temperature. At  $80\text{ }^\circ\text{C}$ ,  $88.9\text{ mmol}$  of carbon dioxide was released in gas phase which indicates that most initial calcium carbonate introduced in the reactor ( $100\text{ mmol}$ ) was decomposed.

The filtrate recovered from the reaction mixture was acidified with concentrated nitric acid to avoid any further precipitation or transformation of calcium cations with orthophosphate and/or carbonate anions. Then, dissolved calcium and phosphorus contents in the filtrate were analyzed by ICP-AES technique. In all cases, there was less than

**Table 1**  
IR peak positions and corresponding assignment [19–22]; Y and N: with and without the presence of absorption band, respectively.

Wavelength, $\text{cm}^{-1}$	Solid				Assignment
	20 °C	40 °C	60 °C	80 °C	
3600	Y	Y	Y	Y	O–H (water), $\nu_1$ mode
1645	Y	Y	Y	N	H–O–H, $\nu_3$ mode
1545	N	N	Y	Y	C–O, $\nu_3$ mode
1450	N	N	Y	Y	C–O, $\nu_3$ mode
1415	N	N	Y	Y	C–O, $\nu_3$ mode
1296	Y	Y	Y	N	P–(OH) stretching
1194	Y	Y	Y	N	P–(OH) stretching
1120	Y	Y	N	N	$\text{PO}_4$ , $\nu_3$ mode
1076	Y	Y	Y	N	$\text{PO}_4$ , $\nu_3$ mode
1055	Y	Y	Y	N	$\text{PO}_4$ , $\nu_3$ mode
1038	Y	Y	Y	N	$\text{PO}_4$ , $\nu_3$ mode
1018	Y	Y	Y	Y	$\text{PO}_4$ , $\nu_3$ mode
960	Y	Y	Y	Y	$\text{PO}_4$ , $\nu_1$ mode
916	Y	Y	Y	N	$\text{HPO}_4$ , $\nu_4$ mode
870	Y	Y	Y	Y	C–O, $\nu_2$ mode (B-type CAPs or calcite)
880	N	N	Y	Y	C–O, $\nu_2$ mode (A-type CAPs)
711	Y	Y	Y	N	C–O, $\nu_4$ mode
633	Y	Y	Y	Y	O–H (Ca-HA), libration $\text{HPO}_4$ , $\nu_4$ mode
603	Y	Y	Y	Y	$\text{PO}_4$ , $\nu_4$ mode
559	Y	Y	Y	Y	$\text{PO}_4$ , $\nu_4$ mode
530	Y	Y	Y	N	$\text{HPO}_4$ , $\nu_4$ mode

1% of the initial calcium and phosphorus introduced in the reactor which existed in soluble forms. This means that the precipitation of orthophosphoric acid into solid calcium phosphates was complete and

all calcium cations released from Eq. (1) completely re-precipitated too. ICP-AES analysis of the bulk solids after mineralization with concentrated nitric acid showed that the molar ratio of Ca/P was about 1.8. This is slightly higher than the stoichiometric value of Ca-HA and will be discussed in more details in the NMR and IR characterizations section.

The content of residual calcium carbonate in the solid products was quantified by TG analysis (Section 3.4) and the obtained results are reported in Fig. 2. As expected, the decomposition of calcium carbonate increased with the increase of reaction temperature. At 80 °C, the disappearance of calcium carbonate was nearly complete after 48 h of reaction.

The solid products were then characterized by different physico-chemical techniques to identify the intermediates present.

### 3.2. XRD characterization

XRD characterization was performed in order to investigate the crystalline phases present in the solid products using JCPDS standards. The results are presented in Fig. 3.

As shown in Fig. 3, unreacted calcium carbonate, having the main diffraction peak at 29.40°, was clearly observed in the solid products synthesized within the reaction temperature range of 20–60 °C. On the other hand, only trace amounts of this starting reactant was observed in the solid product obtained at 80 °C which confirmed the favorable effect of the reaction temperature on the decomposition of initial calcium carbonate particles. The yield of calcium carbonate decomposition strongly influenced the crystalline structure of the solid calcium phosphates formed. When the decomposition of calcium carbonate was nearly complete (80 °C), all diffraction peaks could be

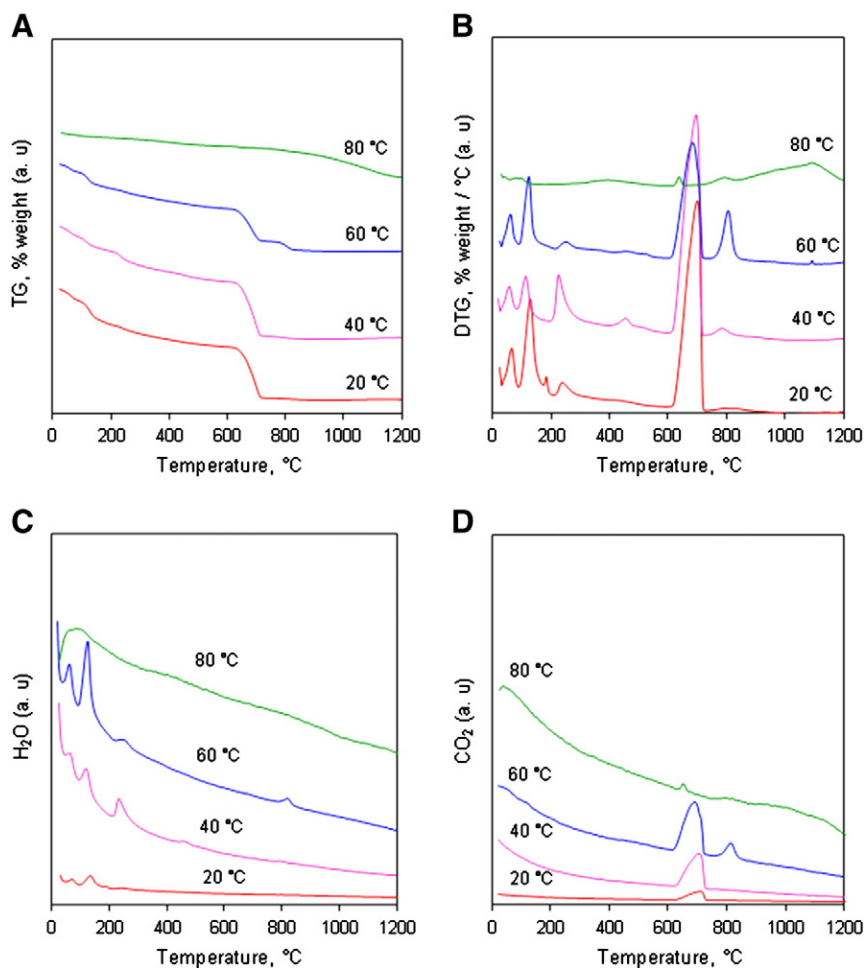


**Fig. 6.** TG (A) and DTG (B) curves of the solid products dried at 55 °C; evolution of H<sub>2</sub>O (C) and CO<sub>2</sub> (D) in gas phase during TG analysis.

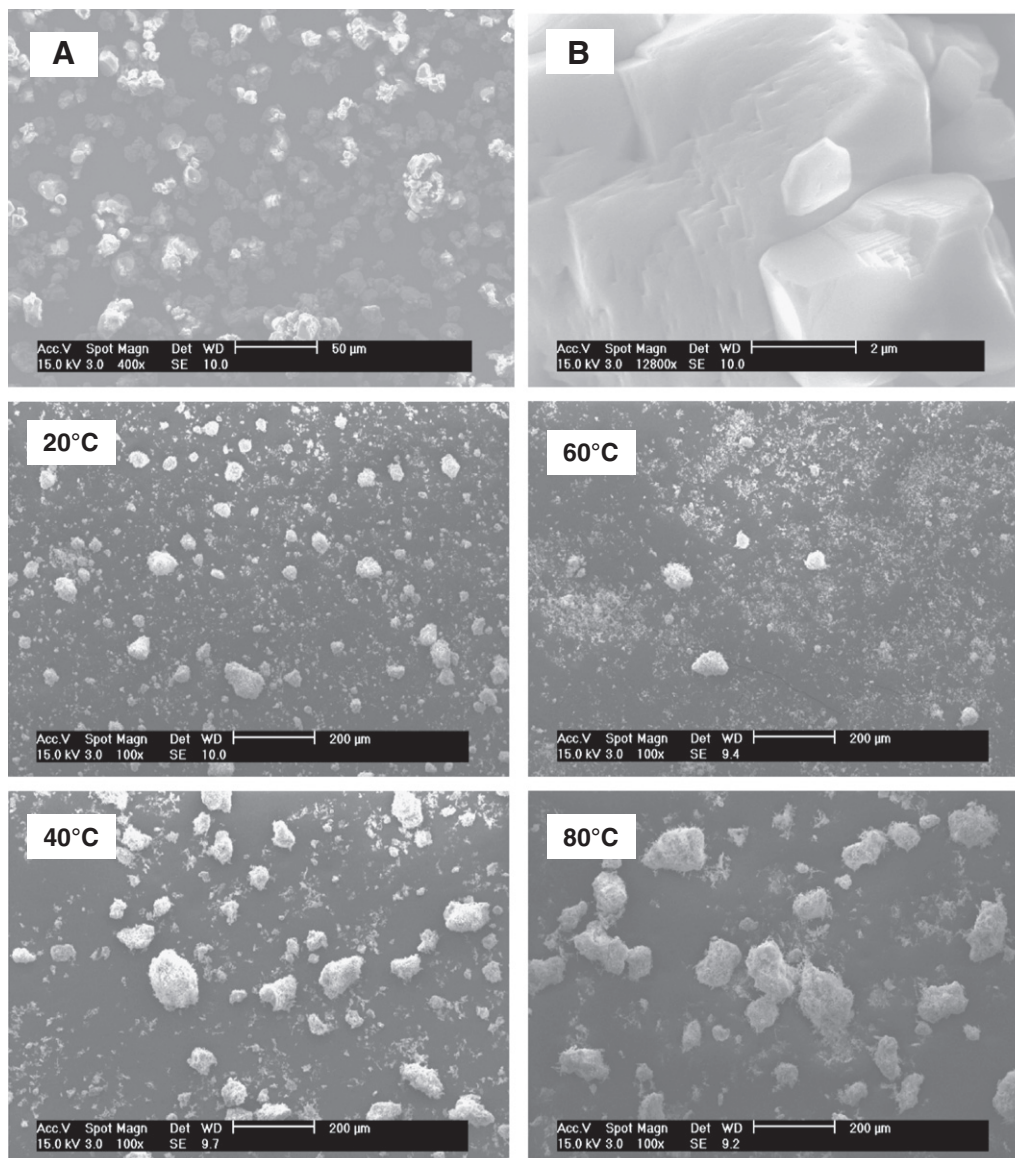


Fig. 7. SEM micrographs of solid calcium phosphate products at low magnification (20–80 °C) and the initial calcium carbonate (A and B).

attributed to Ca-HA (JCPDS standard no. 01-072-1243) and calcium carbonate-containing apatites of both B-type (JCPDS standards nos. 00-019-0272 and 00-004-0697) and A-type (JCPDS standard no. 00-035-0180), labeled thereafter CAPs. However, it was difficult to distinguish these apatitic compounds because their main diffraction peaks are all in the 2 theta range of 31.5–31.8°.

When the dissociation of calcium carbonate was incomplete (20–60 °C), different calcium phosphates co-existed. Octacalcium bis(hydrogenphosphate) tetrakis(phosphate)pentahydrate (OCP,  $\text{Ca}_8(\text{HPO}_4)_2(\text{PO}_4)_4 \cdot 5\text{H}_2\text{O}$ ), which has the main diffraction peak at 2 theta of 4.7°, was the main apatitic calcium orthophosphate. Its signal decreased with the increase of the reaction temperature indicating its transformation into more stable apatites. Ca-HA, which has the main diffraction peak at 2 theta of 31.7°, was also formed but with low crystallinity as shown by its weak broad peaks. Other calcium orthophosphates such as CAPs, dicalcium phosphate anhydrous (DCPA, JCPDS standard no. 00-003-0398) could be also present at much lower contents.

In all cases, the final pH of the reaction mixture was around 8, which was favorable for the formation of apatitic compounds.

### 3.3. NMR and IR characterizations

To enhance the results of XRD characterization, NMR and IR analyses of the solid products were investigated. Fig. 4(A) presents the  $^{31}\text{P}$  NMR spectra of the dried solid products. The three solid products obtained at 20, 40 and 60 °C showed four characteristic chemical shifts of OCP [16]. On the other hand, the solid product synthesized at 80 °C showed only one chemical shift at 3.7 ppm, which was characteristic for Ca-HA based products [17].

Fig. 4(B) shows the  $^1\text{H}$  NMR spectra of the dried solid products. The chemical shift at about 13 ppm was characteristic for the  $\text{HPO}_4^{2-}$  ions located in the apatitic layer of the OCP's structure [18]. This shift appeared only in the solid products synthesized at 20–60 °C with uncompleted dissociation of calcium carbonate, and was not found in the product synthesized at 80 °C with complete conversion of calcium carbonate. The shift at about -0.1 ppm was characteristic for  $\text{OH}^-$  ions present in Ca-HA's structure [17]. This peak was much more intense in the product synthesized at 80 °C than in the other products. All these results confirmed those of XRD analysis, that OCP and Ca-HA were the main components of the solid products synthesized at

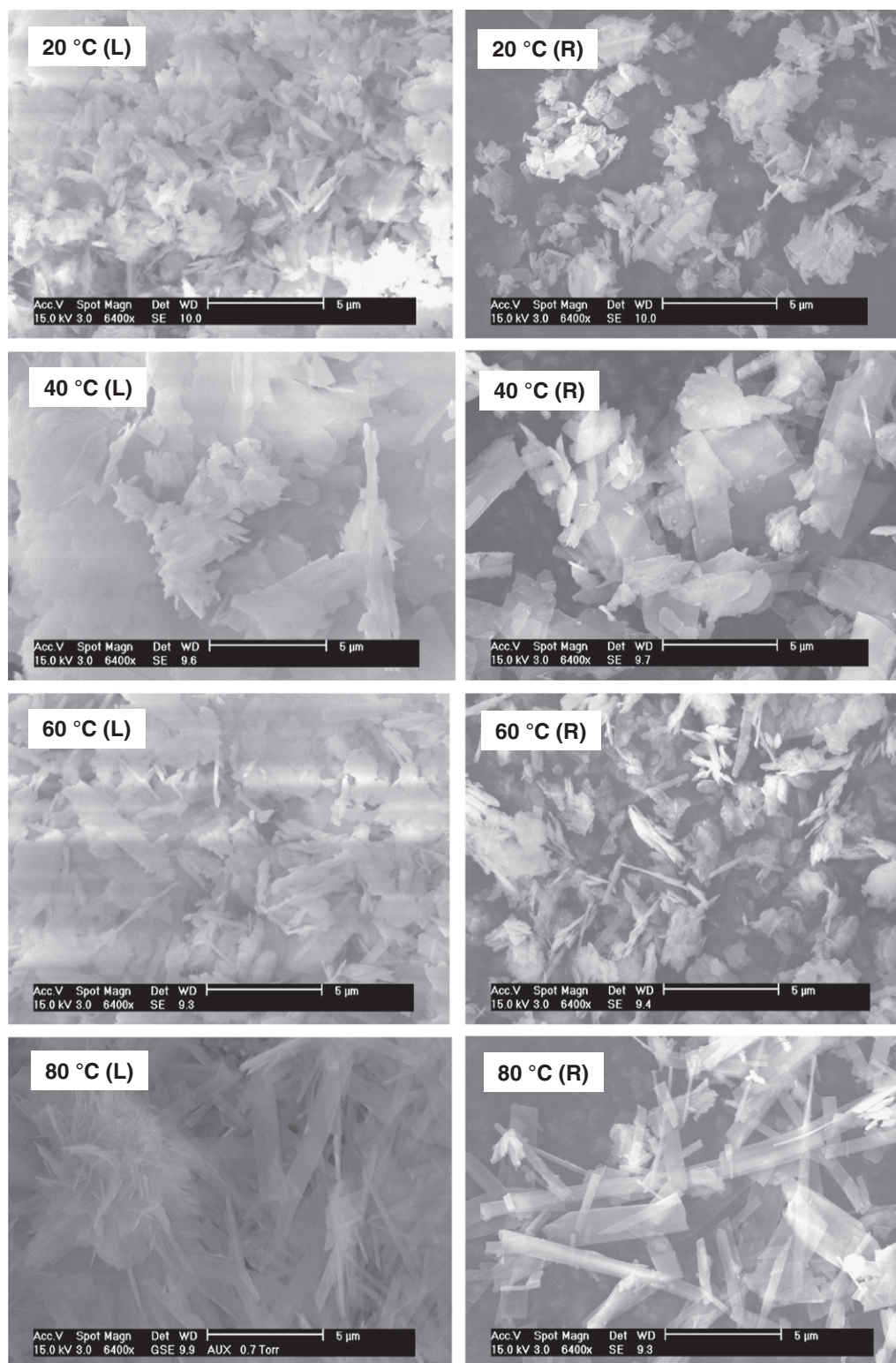


**Fig. 8.** SEM micrographs of large particles (left-hand side, L) and smaller particles (right-hand side, R).

20–60 °C and 80 °C, respectively. Finally, the peak with chemical shift at about 5 ppm (Fig. 4(B)) could be attributed to adsorbed water, which was present in all four solid products [19].

Fig. 5 shows IR spectra of all four solid products, and most significant peaks in the wavelength range of 4000–500  $\text{cm}^{-1}$  are summarized in Table 1. In the wavelength range of 4000–1700  $\text{cm}^{-1}$ , there was only

a weak broad peak at about 3600–3000  $\text{cm}^{-1}$  (not presented), which was assigned to O–H stretching of molecular water.

According to the results of XRD analysis, the remaining calcium carbonate in the solid products was characterized by the peak at 711  $\text{cm}^{-1}$ , which was not present in the solid obtained at 80 °C. This last one also lacked the peak at 1645  $\text{cm}^{-1}$ , assigned to

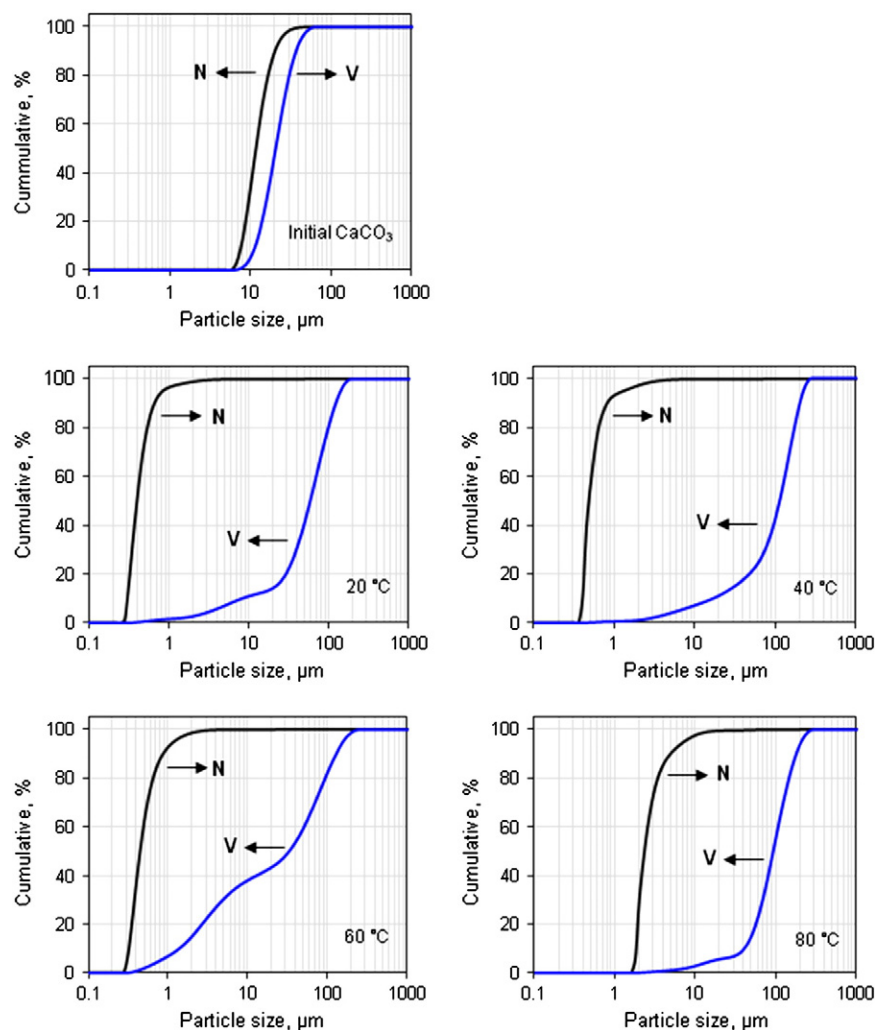


Fig. 9. Particle size distribution by number (N) or volume (V) of particles (particle size is in base 10 logarithmic scale).

H–O–H bending of molecular water in the structure of OCP, which confirmed the absence of OCP as shown by XRD (Fig. 3). The weak absorption band at  $633\text{ cm}^{-1}$ , assigned to the vibrational mode of  $\text{OH}^-$  groups indicated the presence of stoichiometric Ca-HA. The bi-modal peak at  $1450\text{ cm}^{-1}/1415\text{ cm}^{-1}$  and the peak at  $870\text{ cm}^{-1}$  were characteristic for B-type CAPs (replacement of  $\text{PO}_4^{3-}$  groups by  $\text{CO}_3^{2-}$  groups). On the other hand, A-type CAPs (replacement of  $\text{OH}^-$  groups by  $\text{CO}_3^{2-}$  groups) were characterized by the peaks at  $1545\text{ cm}^{-1}$  and  $880\text{ cm}^{-1}$ . Thus, B-type CAPs could be present in all four solid products while A-type CAPs could only be found in the solids obtained at  $60\text{ }^\circ\text{C}$  and  $80\text{ }^\circ\text{C}$ . So, the increase of reaction temperature was favorable for both the decomposition of calcium carbonate and the formation of CAPs, particularly A-type CAPs. The presence of B-type CAP explained why the molar ratio of Ca/P of the bulk solids was slightly higher the stoichiometric value of pure Ca-HA. Finally, the absorption bands in the wavelength ranges of  $650\text{--}500\text{ cm}^{-1}$  and  $1300\text{--}910\text{ cm}^{-1}$  were assigned to the vibrations of orthophosphate groups. Classical vibration bands of  $\text{HPO}_4^{2-}$  groups in OCP structure and  $\text{PO}_4^{3-}$  in Ca-HA or CAP structure could clearly be observed.

### 3.4. TG–MS coupling

The thermal behavior of the solid products was investigated using TG analysis. TG and DTG curves obtained in the temperature range of  $25\text{--}1200\text{ }^\circ\text{C}$  are shown in Fig. 6(A) and (B), and the formation of

water and carbon dioxide during the thermal analysis, which was qualitatively measured by MS analysis, are presented in Fig. 6(C) and (D).

All changes in mass as a function of heating temperature could be attributed to the decarbonation and dehydration which were well confirmed by MS analysis. The thermal decomposition of OCP, which was the principal intermediate, is generally complex with different dehydrations in the temperature ranges of  $30\text{--}80\text{ }^\circ\text{C}$ ;  $80\text{--}170\text{ }^\circ\text{C}$  and  $200\text{--}300\text{ }^\circ\text{C}$  [23]. These weight losses were not observed for the solid synthesized at  $80\text{ }^\circ\text{C}$  which was in coherence with the result of XRD, NMR and IR characterizations. The first weight loss at  $30\text{--}80\text{ }^\circ\text{C}$  was attributed to the elimination of physically absorbed surface moisture which should not be significant after drying. The weight loss at  $170\text{--}200\text{ }^\circ\text{C}$ , which was only observed for the solid synthesized at  $20\text{ }^\circ\text{C}$ , could be due to the dehydration of DCPD to form DCPA. This indicated that DCPD could also be an intermediate of the reaction as previously observed in the reaction of limestone with orthophosphoric acid [24]. DCPA was then condensed into calcium pyrophosphate ( $\text{Ca}_2\text{P}_2\text{O}_7$ ) at  $400\text{--}500\text{ }^\circ\text{C}$ . The clearest weight loss at  $600\text{--}720\text{ }^\circ\text{C}$  was due to the decarbonation of residual calcium carbonate. Its content decreased with the increase of reaction temperature, as discussed in Fig. 2. Two next weight losses at  $740\text{--}850\text{ }^\circ\text{C}$  and  $850\text{--}1200\text{ }^\circ\text{C}$  were attributed to the decarbonation and dehydroxylation of CAPs, as accompanied with the release of  $\text{CO}_2$  and  $\text{H}_2\text{O}$ , detected by MS analysis. According to the results of IR analysis, the decarbonation of B-type CAPs, which were present in all four solids, happened at  $740\text{--}850\text{ }^\circ\text{C}$ . On the other hand, the decarbonation of

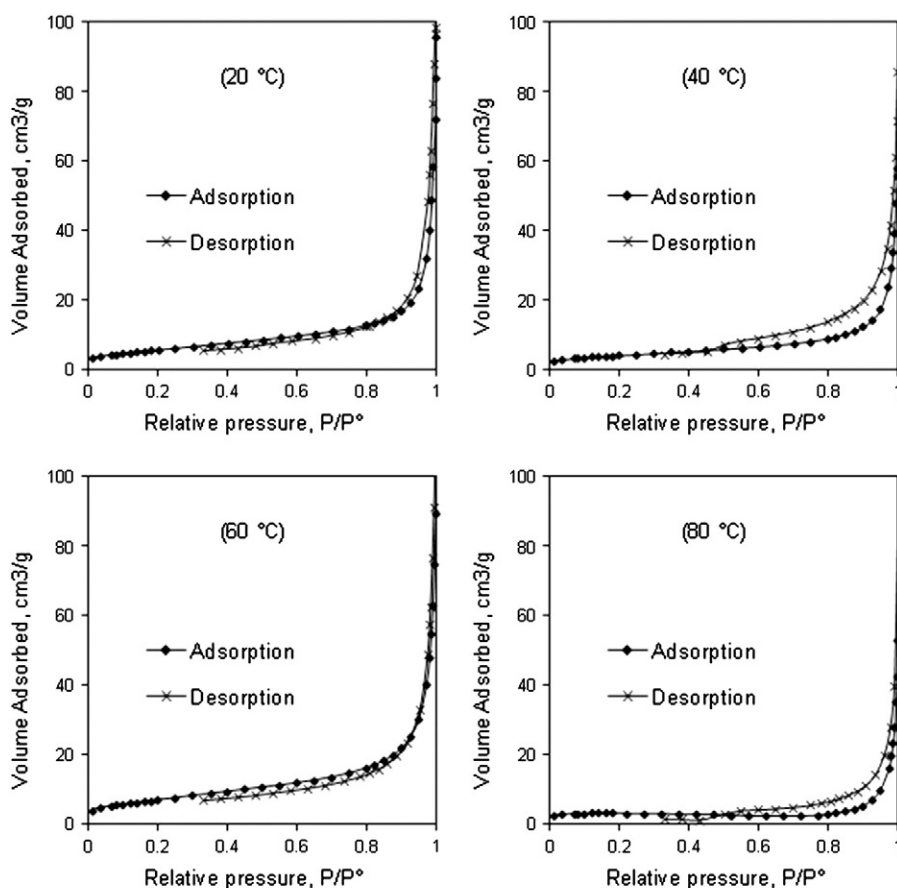


Fig. 10. Adsorption-desorption isotherms of the solid products.

A-type CAPs, which were only formed at 60 °C and 80 °C, occurred at higher temperatures in the range of 850–1200 °C. The decarbonation of the solid synthesized at 80 °C was not finished at 1200 °C which indicated its high thermal stability.

All changes in mass in the temperature range investigated were endothermic as found by differential scanning calorimetry (DSC, not presented).

### 3.5. SEM and particle size distribution

In order to investigate the surface morphology of particles, SEM observation was performed. Fig. 7 presents SEM micrographs of the solid products at low magnification and starting calcium carbonate powder. This initial reactant had a high regularity in particle dimension (Fig. 7(A)) with a smooth and non-porous structure (Fig. 7(B)), which was in coherence with its low specific surface area ( $<2 \text{ m}^2 \text{ g}^{-1}$ ). On the other hand, all four solid products had a variation of particle sizes in large ranges from hundreds of nm to hundreds of  $\mu\text{m}$ , as usually observed previously [25–27].

**Table 2**  
Specific surface area ( $S_{\text{BET}}$ ) and true density ( $D$ ) of the solid products.

Product	$S_{\text{BET}}, \text{m}^2 \text{ g}^{-1}$	$D, \text{g cm}^{-3}$
Initial $\text{CaCO}_3$	<2	2.675
Product at 20 °C	15	2.670
Product at 40 °C	14	2.677
Product at 60 °C	25	2.784
Product at 80 °C	12	2.991

Fig. 8 presents SEM micrographs of particles larger than 50  $\mu\text{m}$  (L) and smaller than 5  $\mu\text{m}$  (R) at the same magnification of 6400 times (5  $\mu\text{m}$  scale). For all solid products, large particles seem to be a result of agglomeration of corresponding fine particles. This has been observed for the precipitation of calcium orthophosphates in aqueous solution [28–30]. Taking into account the rapid increase of pressure in the batch reactor during the first minute of reaction, it is assumed that the first step of the reaction must be the decomposition of calcium carbonate particles in acid medium, accompanied by the release of carbonic gas and the precipitation of calcium cations ( $\text{Ca}^{2+}$ ) by orthophosphate species to form primary fine calcium phosphate particles at nanometric scale. Then, primary fine calcium phosphate particles agglomerated during the reaction time to form larger particles.

Change in morphology of particles as a function of reaction temperature can also be observed in Fig. 8. On the left-hand side, larger aggregates seem to have a porous structure. On the right-hand side, primary particles had a compact appearance and at higher magnification, no macro-pores could be observed (Supplementary data 1). At 20 °C, particles of sheet structure frequently appeared. They seemed to be more numerous at 40 °C and could be attributed to OCP particles [21,31] which were in coherence with XRD results (Fig. 3). Some needle-like particles also appeared at these temperatures. At 60 °C, the frequency of particles of sheet structure decreased and that of needle-like particles considerably increased. Particularly, the change was distinct at 80 °C where most particles were of flat-needle-like morphology (more details in Supplementary data 2). This morphology was characteristic for apatitic compounds formed under hydrothermal conditions, as observed in previous works [32–34].

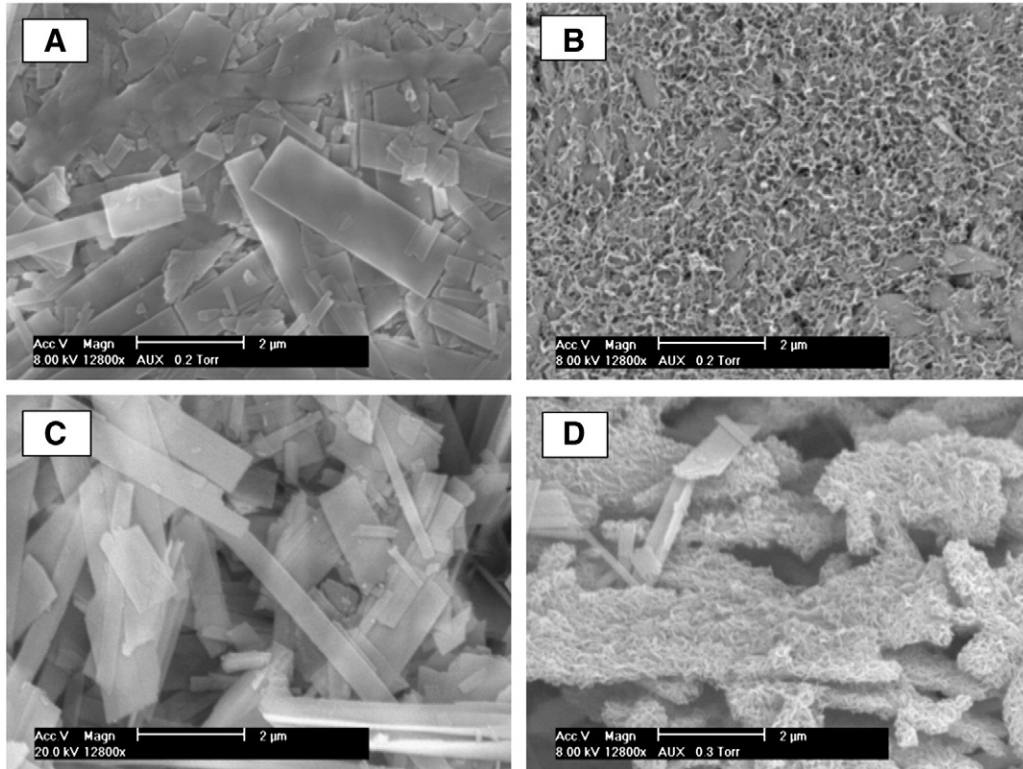


**Fig. 11.** SEM images of CAP synthesized at 80 °C: (A) disk just prepared; (B) disk after soaking in Tris-SBF-27 mM solution at 37 °C for 7 days; (C) dried CAP powder; and (D) CAP powder after soaking in Tris-SBF-27 mM solution at 37 °C for 7 days.

Particle size distribution was also analyzed in order to better understand the formation of particles (Fig. 9).

According to the observation in Fig. 7(A), starting calcium carbonate had a narrow particle size distribution from 7 μm to 50 μm. On the other hand, solid calcium phosphate products showed large ranges of particle sizes from about 0.2 μm to about 270 μm. For the solid products synthesized at 20–60 °C, there was more than 93% of number of particles found in the range of 0.2 μm to 1 μm. On the other hand, the volumes corresponding to this fraction of particle size were found at less than 7%. For the solid synthesized at 80 °C, 97% of the number of particles was found in the range of 1.5 to 10 μm, which corresponded to only 3% of cumulative volume. This means that a deep agglomeration of fine particles took place during the synthesis under the conditions investigated.

### 3.6. Adsorption–desorption isotherm measurements and true density

SEM micrographs at high magnification showed that large solid particles could have macro-pores but this technique did not allow the observation of smaller pore sizes. To better understand the porosity of the obtained materials, adsorption–desorption isotherm measurements were carried out. Fig. 10 shows isotherm plots for the reaction products.

All four solids showed similar adsorption–desorption isotherms of type II solids according to the IUPAC classification of physisorption isotherms [35]. These results indicate that the solid products had only macro-porous structure which confirmed the results of SEM observation.

From the results of isotherm measurements, specific surface areas were obtained using BET method ( $S_{\text{BET}}$ ). True density was measured also and the results are presented in Table 2.

The two solid products synthesized at 20 °C and 40 °C had the same specific surface area, in agreement with similar chemical composition with about 20–22% of the remaining calcium carbonate. At 60 °C, the decomposition of calcium carbonate was more advanced (Fig. 2) and

the resulting solid had a higher specific surface area. At 80 °C, despite a complete decomposition of calcium carbonate, the specific surface area of the reaction product was smallest, which was due to the formation of larger particles by agglomeration (Fig. 9). In parallel with the increase of the reaction temperature, the reaction evolved to apatitic phases which were generally denser than the initial calcium carbonate [36]. This explains the increase of true density as a function of reaction temperature. Clogged porosity may be also formed during the precipitation of apatitic compounds since carbon dioxide was released from the decomposition of calcite. This porosity may be destroyed with the increase of the temperature leading to denser products.

### 3.7. Bioactivity test

SEM observations showed the CAP disks to be composed of flat-needle-like crystals of approximately one micrometer width and several micrometers length (Fig. 11). Following incubation in Tris-SBF-27 mM, the crystals were covered by new calcium phosphate deposits resembling those described in earlier works [15,37]. The underlying CAP crystals can hardly be recognized in Fig. 11(B). The non-compacted crystals are loosened in Fig. 11(D) as a result of water rinsing. Kokubo et Takadama [38] described the formation of such coatings as related to surface bioactivity appropriate for bone bonding activity. Possible improvements of the proposed bioactivity test have been proposed [39].

### 3.8. Discussion

In all our reactions using calcium carbonate and orthophosphoric acid as starting reactants, only traces of soluble calcium cations and orthophosphate species were observed to be present in the liquid phase. This indicates that orthophosphate species precipitated from solution into poorly soluble solid phases. The decomposition of calcium carbonate was also complete at 80 °C after 48 h of reaction. This resulted in the

**Table 3**  
Carbonate contents (CO<sub>2</sub> wt.%) determined from TG curves.

Solid	Decarbonation (CO <sub>2</sub> wt.%)		
	B-type CAP form (740–850 °C)	A-type CAP form (850–1250 °C)	CaCO <sub>3</sub> form (600–720 °C)
20 °C	0.27	0	9.20
40 °C	0.49	0	9.77
60 °C	1.52	0.01	5.41
80 °C	0.76	4.05 <sup>a</sup>	0.18

<sup>a</sup> From TG–MS coupling analysis in the temperature range of 25–1350 °C for a complete decarbonation of the product synthesized at 80 °C (Supplementary data 3).

final formation of “pure apatitic products” which did not require further washing for the elimination of soluble counter ions. This represents real advantages of the present synthesis process in comparison with other routes for CAP synthesis, discussed in the Introduction section [12–14], since water-rinsing is usually a limiting step for the purification of powder products.

From TG curves, the carbonate contents in apatitic structure or in CaCO<sub>3</sub> form could be both estimated quantitatively (Table 3). In parallel with the decomposition of the initial calcium carbonate, the carbonate content (CO<sub>2</sub> wt.%) of CAP increased. The formation of A–B-type CAP (replacement of both PO<sub>4</sub><sup>3-</sup> and OH<sup>-</sup> groups by CO<sub>3</sub><sup>2-</sup> groups) was favorable at 80 °C, where the reaction reached the complete decomposition of starting calcium carbonate.

#### 4. Conclusions

One-step synthesis of carbonate-containing apatite (CAP) has been investigated under moderate conditions, using calcium carbonate and orthophosphoric acid as ubiquitous starting materials. Simple and well known starting materials are advantageous for pharmaceutical productions. The reaction temperature was found to be the key parameter for both the decomposition of initial calcium carbonate particles and the formation of CAP. At 80 °C, which was lower than most hydrothermal conditions, the decomposition of calcium carbonate was complete. At this temperature, the final solid product was composed of only apatitic phases including Ca-HA and A–B type CAP. At lower temperatures, other calcium phosphate phases were formed, in particular OCP. In all cases, only traces of soluble calcium cations and orthophosphate species were found, which shows the complete transformation of the starting materials into the desired product. Carbon dioxide, formed in gas phase, was the only by-product of the synthesis process. CAP obtained at 80 °C was found to be bioactive for the growth of calcium phosphate on its surface after soaking in a simulated body fluid (Tris–SBF–27 mM).

Supplementary data to this article can be found online at <http://dx.doi.org/10.1016/j.msec.2013.03.023>.

#### Acknowledgments

The authors gratefully acknowledge our colleagues, Nathalie Lyczko, Christine Rolland, Sylvie Delconferro, Philippe Accart and Yannick Coppel, for the different characterization measurements.

#### References

- [1] R. Murugan, S. Ramakrishna, K. Panduranga Rao, *Mater. Lett.* 60 (2006) 2844.
- [2] H. Morgan, R.M. Wilson, J.C. Elliott, S.E.P. Dowker, P. Anderson, *Biomaterials* 21 (2000) 617.
- [3] K. Onuma, *Prog. Cryst. Growth Charact. Mater.* 52 (2006) 223.
- [4] C.V.M. Rodrigues, P. Serricella, A.B.R. Linhares, R.M. Guerdes, R. Borojevic, M.A. Rossi, M.E.L. Duarte, M. Farina, *Biomaterials* 24 (2003) 4987.
- [5] E.S. Thian, Z. Ahmad, J. Huang, M.J. Edirisinghe, S.N. Jayasinghe, D.C. Ireland, R.A. Brooks, N. Rushton, W. Bonfield, S.M. Best, *Biomaterials* 29 (2008) 1833.
- [6] Y. Doi, T. Shibutani, Y. Moriwaki, T. Kajimoto, Y. Iwayama, *J. Biomed. Mater. Res.* 39 (4) (1998) 603.
- [7] M.E. Fleet, X. Liu, *Biomaterials* 26 (2005) 7548.
- [8] I. Khattech, M. Jemal, *Thermochim. Acta* 95 (1985) 119.
- [9] J.P. Lafon, E. Champion, D. Bernache-Assollant, *J. Eur. Ceram. Soc.* 28 (2008) 139.
- [10] F. Bel Hadj Yahia, M. Jemal, *Thermochim. Acta* 505 (2010) 22.
- [11] J.C. Elliott, *Studies in Inorganic Chemistry 18: Structure and Chemistry of the Apatites and Other Calcium Orthophosphates*, Elsevier, Amsterdam–London–New York–Tokyo, 1994. 191–199.
- [12] M.E. Fleet, *Biomaterials* 30 (2009) 1473.
- [13] M.E. Fleet, X. Liu, *J. Solid State Chem.* 174 (2003) 412.
- [14] L.M. de Oliveira, A.M. Rossi, R.T. Lopes, *Radiat. Phys. Chem.* 61 (2001) 485.
- [15] S. Jalota, S.B. Bhaduri, A.C. Tas, *Mater. Sci. Eng. C* 28 (2008) 129.
- [16] Y.H. Tseng, J. Zhan, K.S.K. Lin, C.Y. Mou, J.C.C. Chan, *Solid State Nucl. Magn. Reson.* 26 (2004) 99.
- [17] C. Jager, T. Welzel, W. Meyer-Zaika, M. Epple, *Magn. Reson. Chem.* 44 (2006) 573.
- [18] J.C. Elliott, *Studies in Inorganic Chemistry 18: Structure and Chemistry of the Apatites and Other Calcium Orthophosphates*, Elsevier, Amsterdam–London–New York–Tokyo, 1994. 21–22.
- [19] R.M. Wilson, J.C. Elliott, S.E.P. Dowker, R.I. Smith, *Biomaterials* 25 (2004) 2205.
- [20] B. Mihailova, B. Kolev, C. Balarew, E. Dyulgerova, L. Konstantinov, *J. Mater. Sci.* 36 (2001) 4291.
- [21] R. Horvathova, L. Muller, A. Helebrant, P. Greil, F.A. Muller, *Mater. Sci. Eng. C* 28 (2008) 1414.
- [22] A. Antonakos, E. Liarokapis, T. Leventouri, *Biomaterials* 28 (2007) 3043.
- [23] J.C. Elliott, *Studies in Inorganic Chemistry 18: Structure and Chemistry of the Apatites and Other Calcium Orthophosphates*, Elsevier, Amsterdam–London–New York–Tokyo, 1994. 9–29.
- [24] D.W. Kim, I.S. Cho, J.Y. Kim, H.L. Jang, G.S. Han, H.S. Ryu, H. Shin, H.S. Jung, H. Kim, K.S. Hong, *Langmuir* 26 (1) (2010) 384.
- [25] M. Yoshimura, P. Sujaridworakun, F. Koh, T. Fujiwara, D. Pongkao, A. Ahniyaz, *Mater. Sci. Eng. C* 24 (2004) 521.
- [26] W.L. Suchanek, P. Shuk, K. Byrappa, R.E. Riman, K.S. TenHuisen, V.F. Janas, *Biomaterials* 23 (2002) 699.
- [27] Y. Guo, Y. Zhou, D. Jia, H. Tang, *Microporous Mesoporous Mater.* 118 (2009) 480.
- [28] R. Rodriguez-Clemente, A. Lopez-Macipe, J. Gbmez-Morales, J. Torrent-Burges, V.M. Castaño, *J. Eur. Ceram. Soc.* 18 (1998) 1351.
- [29] R. Morsya, M. Elsayed, R. Krause-Rehberg, G. Dlubek, T. Elnimr, *J. Eur. Ceram. Soc.* 30 (2010) 1897.
- [30] W.L. Suchanek, K. Byrappa, P. Shuk, R.E. Riman, V.F. Janas, K.S. TenHuisen, *J. Solid State Chem.* 177 (2004) 793.
- [31] S. Ishihara, T. Matsumoto, T. Onoki, T. Sohmura, A. Nakahira, *Mater. Sci. Eng. C* 29 (2009) 1885.
- [32] M.I. Dominguez, J. Carpena, D. Borschnek, M.A. Centeno, J.A. Odriozola, J. Rose, *J. Hazard Mater.* 150 (2008) 99.
- [33] A. Kasiopas, T. Geisler, C. Perdikouri, C. Trepmann, N. Gussone, A. Putnis, *Geochim. Cosmochim. Acta* 75 (2011) 3486.
- [34] K. Ioku, S. Yamauchi, H. Fujimori, S. Goto, M. Yoshimura, *Solid State Ionics* 151 (2002) 147.
- [35] K.S.W. Sing, D.H. Everett, R.A.W. Haul, L. Moscou, R.A. Pierotti, J. Rouquerol, T. Siemieniowska, *Pure Appl. Chem.* 57 (4) (1985) 603.
- [36] H. Morga, R.M. Wilson, J.C. Elliott, S.E.P. Dowker, P. Anderson, *Biomaterials* 21 (2000) 617.
- [37] Y.R. Duan, Z.R. Zhang, C.Y. Wang, J.Y. Chen, X.D. Zhang, *J. Mater. Sci. Mater. Med.* 15 (2004) 1205.
- [38] T. Kokubo, H. Takadama, *Biomaterials* 27 (2006) 2907.
- [39] M. Bohner, J. Lemaitre, *Biomaterials* 30 (2009) 2175.